Scanning Microscopy

Volume 1993
Number 7 *Physics of Generation and Detection of Signals Used for Microcharacterization*

Article 19

1993

Surface Chemical Reactions at the Atomic Scale: Gas Reactions with Semiconductors Studied with Scanning Tunneling Microscopy

R. S. Becker
AT&T Bell Laboratories

Y. J. Chabal
AT&T Bell Laboratories

G. S. Higashi
AT&T Bell Laboratories

A. J. Becker
AT&T Bell Laboratories

Scanning Microscopy Supplement 7, 1993 (Pages 269-280) 0892-953X/93$5.00+.25
Scanning Microscopy International, Chicago (AMF O'Hare), IL 60666 USA

SURFACE CHEMICAL REACTIONS AT THE ATOMIC SCALE: GAS REACTIONS WITH SEMICONDUCTORS STUDIED WITH SCANNING TUNNELING MICROSCOPY

R.S. Becker[1], Y.J. Chabal*, G.S. Higashi, A.J. Becker

AT&T Bell Laboratories, Murray Hill, NJ 07974
[1]Current address: Rural Route 3, Box 1300, Lebanon, IA 17046

Abstract

The vacuum tunneling microscope has been extensively utilized in the study of the surface atomic configuration of conducting materials. Analysis of features in both the tunneling images and in the tunnel junction I-V characteristic yields insight into a wide variety of processes occurring at surfaces. In the last few years, elementary chemical reactions occurring at surfaces have been examined in this manner, principally adsorption of simple gas species such as H_2, O_2, and NH_3 on semiconductors and metals. Adsorption sites have been deduced from changes brought about in surface configuration subsequent to gas exposure. The relationship of these sites with one another and their evolution as a function of exposure has been utilized to constrain mechanisms for the adsorption process.

More recently, work has been performed where the scanning tunneling microscope (STM) takes on an active role. Hydrogen terminated silicon surfaces have been prepared and imaged with the STM. The tunneling images and infrared absorption spectra showed that configurations of both the terraces and steps are radically changed due to hydrogen capping. Moreover, the low-energy high-current density electron source, which is formed by the STM tip, has been used to selectively desorb this species from the surface. This process results in configuration changes which are derived from both the desorption kinetics and the long-range configuration of the initial surface.

Key Words: Scanning tunneling microscope, reaction sites, electron stimulated desorption.

*Address for correspondence:
Y.J. Chabal,
AT&T Bell Laboratories,
600 Mountain Avenue,
Murray Hill, New Jersey, 07974.
Phone No.: (908) 582 4193
Fax No.: (908) 582 3901

Introduction

Historically, scientists have had to be content in viewing and understanding the basic interactions and reactions between materials from a macroscopic standpoint, using statistical mechanics to describe the complex relations between interacting species. Ultimately, one would like to view these processes on a microscopic, if not atomic scale, employing a quantum mechanical framework to describe processes atom by atom and molecule by molecule. For the subset of processes that occur at or very near surfaces, a new tool, the scanning tunneling microscope (STM), may be used to both image and stimulate surface systems on an atomic scale. In the ten years since its development, the STM has already been extensively employed in imaging the surface atomic configurations of a large variety of conducting and semiconducting materials.

Going beyond the study of clean surfaces, pioneering ground has already been broken in the study of small amounts of adsorbates on clean surfaces. The adsorption and dissociation of simple molecules on clean surfaces is one of the simplest reactions in nature, yet a thorough understanding of the sequence of events in these systems has eluded many experiments. One of the more fundamental questions is the site or sites for adsorption, for even simple surfaces may exhibit a number of different reaction sites. Even the most carefully prepared starting surface contains fundamental defects, such as steps, which may aid or hinder the adsorption process. For elemental materials, surface atoms can have an atomic configuration that is different from the bulk atoms leading to the formation of domains and domain boundaries. There may also be point defects such as missing or foreign atoms. For multi-component materials, all of the above may occur together with the fact that the constituent elements may have quite different reactivities. In this area, the STM has a considerable advantage over diffraction methods since the formation of tunneling images is not dependent on the long-range order of the surface. Another area of basic interest concerns reactions occurring after surface contact. To this end, some knowledge of the relative charge state of

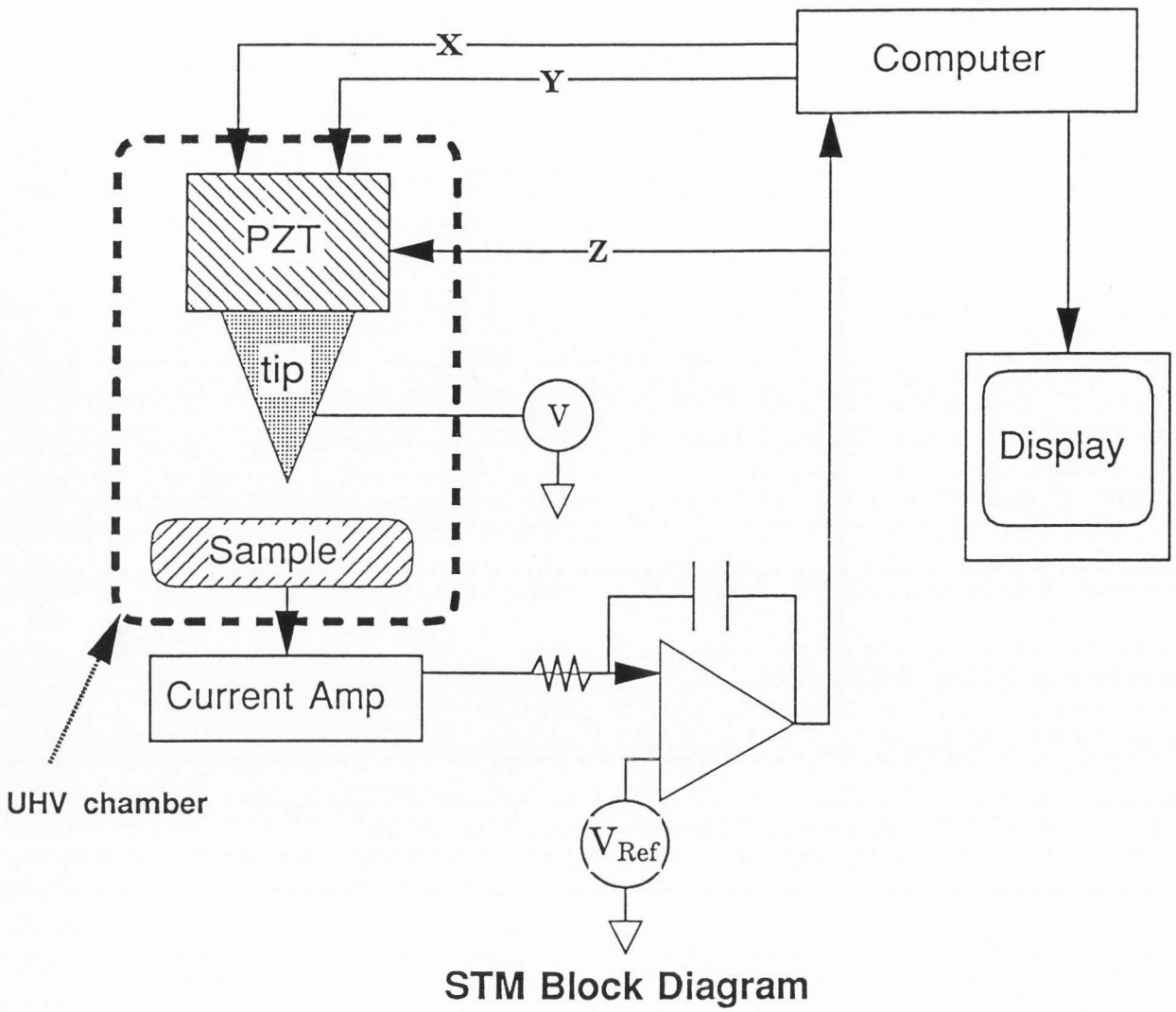

Figure 1. Schematic diagram of a typical vacuum scanning tunneling microscope showing the relationship of the transducers, feedback electronics, computer, and display system.

---

various reacted sites can be obtained by **voltage-dependent imaging** and **tunnel junction spectroscopy**. Under favorable conditions, these enhancements give insight into the nature of the reactions at the various sites.

Beyond passive examination of the reacted surface, the STM may also be used in an active role to stimulate simple processes such as desorption of species from the surface. When operated in the field emission mode, the probe tip serves as a localized electron source with high current density. In this manner, atomic and molecular species may be desorbed from the surface by several mechanisms: local heating, electron stimulated desorption, and, for molecules, electron stimulated dissociation and desorption. This capability has been demonstrated for hydrogen passivated semiconductor surfaces [3]. Continued work on this system indicates that some of the substrate atoms may be rearranged from their passivated configuration during the desorption process.

Method of Operation

When used for imaging, the STM (depicted schematically in Figure 1) may be operated in at least two modes: **constant current imaging** (feedback error mode) or **constant height** (current error mode). Of these two, the former is generally utilized for studies of metals and semiconductors under ultra high vacuum

(UHV) conditions, while the latter is quite common in studies of systems such as graphite and various chalcogenides under ambient conditions. In the **constant current mode**, as shown in Figure 1, the demanded tunneling current, typically 0.1 to 10 nA, is held fixed by a feedback loop which compares the instantaneous tunneling current to a preset value and servos the piezoelectric transducer carrying the tip in or out, varying the tip height so as to maintain this value. A plot of these servo positions (feedback error) against lateral displacement generates a pseudo-topographic plot of the atomic positions. In the **constant height mode**, the bandwidth of the height controlling feedback electronics is reduced so as to maintain a constant average height. The tip is then scanned at a frequency exceeding the loop response; the variations in tunneling current are recorded and plotted against lateral displacement to create a current error image.

It must be stressed that in neither of these modes may the image created by plotting error signal against lateral displacement be simply interpreted as the "heights" of the surface atoms. For the constant current mode, theoretical analysis has shown the tip follows contours of constant local density of states (LDOS), integrated from the sample Fermi level to the tip bias, **at the position of the tip**, which is generally 6-10 Å above the surface [16]. The contours of local state density are derived from both the geometric position of the surface atoms and their electronic structure. In fact, the electronic structure plays a much greater role in determining the apparent heights than does the geometric height. For this reason, images taken under diverse bias conditions may appear quite different as disparate electron states are accessed. For the constant height mode, the analysis is similar with variations in tunneling current reflecting deviations from the average tunneling probability. As the LDOS at the tip position increases, the current rises and similarly falls as the LDOS decreases. A distinct disadvantage of the constant height mode is the difficulty which it has accommodating any but the smoothest surfaces, for even the presence of a step can cause tip-surface contact with generally catastrophic results for both electrodes.

As mentioned, the STM may further be used to irradiate areas of the sample surface from 30 Å to 5 μm in extent with a high-current density ($\sim 10^5$ Å/cm^2), low-energy (0-100 eV) beam of electrons. In this **field emission mode**, the STM may take on an active mode, employing the Coulomb interaction of the electrons with surface atoms and adsorbed species to stimulate processes such as desorption and dissociation. In these experiments, the height controlling feedback loop may be either engaged or disengaged depending on the total current, the electron energy, and the irradiated area. When exposing small areas ($<$ 200 Å extent), the feedback loop is typically engaged while the tip bias is raised to the desired level, held for a predetermined exposure, and then returned to tunneling conditions. For equivalent exposure of larger areas on the scale of microns, the feedback loop is disengaged, the tip is retracted a fixed distance (typically 0.1 to 1.0 μm), the tip bias is raised to the desired level, and the exposure is carried out. The increased tip-sample separation combined with the demand for field emission currents on the scale of 1-10 μA requires electron energies of 50-100 eV. Multiple scattering and secondary electron emission cause the effective illuminated area to increase rapidly beyond that dictated by the separation between the electrodes.

Gas Adsorption on Semiconductors

Adsorption of simple molecular gases on clean surfaces is a basic technique used for many years in surface studies. The STM has been employed to study H_2 and O_2 adsorption on the elemental semiconductors silicon and germanium, as well as the compound semiconductor gallium arsenide. In an early study, Stroscio *et al.* [14] used the STM in both topographic and spectroscopic modes to examine the adsorption of sub-monolayer quantities of oxygen on the cleaved surface of GaAs(110) at room temperature. They found that the appearance of the adsorbed oxygen was a function of the tunneling bias conditions, as may be expected since varying the tip-sample bias (both polarity and magnitude) changes the electron states that the STM accesses. Specifically, the features indicative of adsorbed oxygen appeared higher when tunneling out of occupied sample states and lower than the surrounding GaAs surface when tunneling into unoccupied sample states. This observation is consistent with the electronegativity of oxygen with respect to GaAs; the oxygen accepts a conduction band electron from the GaAs surface, filling the 2p level. This "charging" of the adsorbate causes an excess of occupied state density at the oxygen atom site, while depleting the unoccupied state density in the immediate surroundings since the presence of the additional charge tends to repel conduction band electrons. Depending on the bias polarity, a raised or depressed region was noted around the adsorbate. This effect is purely electronic and is due to the screening by the conduction band electrons which are repelled from the charged adsorbate.

The progressive uptake of oxygen on the Si(111)-7x7 and Ge(111)-c2x8 surfaces has been followed using STM topographic images. The 7x7 surface reconstruction of silicon has been the object of intense study for more than 30 years, with a detailed structure only recently determined [15]. This surface phase consists of twelve adatoms arranged in two groups of six, each

bonded to three substrate atoms. There further exists a partial stacking fault dividing the unit mesh into two halves. Initial experiments on molecular oxygen adsorption on Si(111)-7x7 were performed while the instrument was scanning [7, 17]. This method unfortunately precludes accurate observation due both to the fact that the STM tip occludes the sample surface, rendering measurements of sticking coefficient meaningless, and the high electric field in the tip-sample junction may affect both the adsorbate surface coverage and the dissociation rate in an uncontrolled manner. Nonetheless, these measurements did indicate a reacted Si adatom site which was generally found near defective areas of the silicon sample, suggesting that these may serve as nucleation sites. Following this, a more controlled study by Pelz and Koch [11] revealed that reaction does tend to occur at adatom sites, with at least two different reaction species evident. As the oxygen exposure is increased, reacted adatoms initially manifest themselves as bright, or higher than the surrounding unreacted adatoms. These are referred to as the S_1 state. As time passes, a new reaction state occurs which is manifested as adatoms appearing darker, or lower, than the surrounding adatoms, designated the S_2 state. Again, it must be stressed that the apparent height differences which account for the reacted sites appearing brighter/darker is a reflection of the LDOS, and not the height of the atoms, in general. As the oxygen exposure is increased, more S_2 adatoms are noted, and the bulk of both are located on the faulted half of the 7x7 unit mesh, suggesting increased reactivity at this point, similar to that found in experiments where Pd was deposited at room temperature. Statistics obtained from the images also indicate some preference for corner adatoms over middle adatoms, as was found in studies on NH_3 absorption on Si(111)-7x7 [19]. It is further noted that the spatial distribution for the S_2 final state is more uniform than for the S_1 state, indicating that S_2 may be reached by alternate paths. Without exposure to further amounts of oxygen, this conversion from S_1 to S_2 may be accelerated by gently annealing the sample to $\sim$650°C for short periods of time. No model was suggested that adequately accounted for all of these observations.

The Ge(111)-c2x8 surface is considerably different in atomic geometry than the Si(111)-7x7, consisting of a simple 2x2-like adatom array arranged on a 1x1 surface double-layer [2]. The c2x8 consists of an ordered array of subunits, the 2x2 and c4x2 which are composed of Ge adatoms similar to those found on Si(111)-7x7 but without the-stacking fault. The c2x8 is not as stable as the 7x7; STM topographic studies show that large regions of the surface consist entirely of the component subunits. This lack of a high degree of order has the potential for a large number of possible reaction sites. The disorder on the c2x8 extends to the surface steps, which are ragged and uneven in contrast to the highly reconstructed steps displayed by Si(111)-7x7 [1]. Remarkably, topographic images at successive oxygen exposures at room temperature show that both the c2x8 domains and the steps are relatively unreactive, while the smaller subunits found at c2x8 domain boundaries are the initial reaction sites [6]. As these boundary areas adsorb oxygen, the disorder slowly increases, providing further sites for the uptake of oxygen. These STM observations are consistent with earlier low energy electron diffraction (LEED) studies of this process [8] which show that the c2x8 diffraction pattern persists through quite high exposures of oxygen. The authors suggest that the reactivity of the domain boundaries is related to the increased density of unsatisfied dangling bonds found in these areas due to the unfavorable geometry. Further observations carried out on Ge(111)-c2x8 surfaces exposed to oxygen at temperatures above the c2x8 $\rightarrow$ 1x1 phase transition ($\sim$300°C) show that oxygen has nucleated uniformly over the entire sample surface. This is simply due to the fact that the transition to the "1x1" surface phase is, in reality, a highly disordered adatom phase, effectively rendering the surface as one large domain boundary. The binding of the oxygen at elevated temperature prevents the surface from resuming the c2x8 phase as the sample is cooled.

Electron Stimulated Desorption

Beyond the passive role played by the STM when used to observe the effects of a chemical process at a surface, the device may also take on an active role in the experiment, using the high density electron beam emanating from the tip to stimulate the reaction process. Probably the simplest effect that may occur is the heating of the sample due to the impinging electron beam. Calculations show, depending on the thermal conductivity of the substrate, that temperature rises of several tens of degrees may be expected, causing weakly bound species to diffuse or desorb. Another process that can occur is that of electron stimulated desorption. Here the field-emitted electrons resonantly excite adsorbed species, causing their desorption from the surface, which is subsequently observed with the STM.

In the first experiment of this kind performed with the STM, atomic hydrogen was resonantly desorbed from a Si(111) surface from selected areas of the sample [3]. In this set of experiments, the passivated H-terminated surface was prepared using wet chemical methods [5] and brought into UHV conditions with the STM without further sample treatment. As expected, the Si(111):H surface displayed a 1x1 surface in the

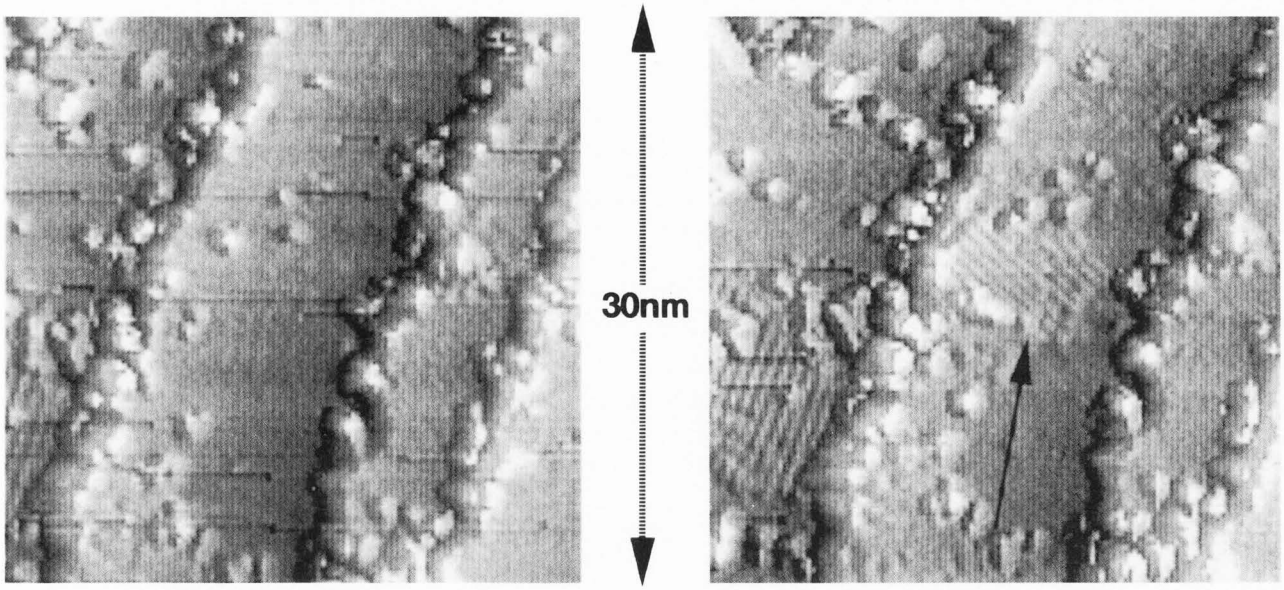

Figure 2. (a) Before and (b) after electron pulse tunneling images of a Si(111):H-1x1 surface showing the creation of a new 2x2 region near the center. A previously created region is visible in the lower left of both images. Two double-layer steps run nearly vertical through the field, with the lateral scale as indicated. These images, and those in the rest of the figures, are constant current topographs displayed as a gray scale, with lighter shades representing higher regions, and darker shades representing lower regions.

---

tunneling images, with apparent high points separated by 3.8 Å along $\langle\bar{1}10\rangle$ surface directions. What was not expected was the observation that the surface reconstruction and electronic characteristics could be transformed from the Si(111):H-1x1 to the Si(111)-2x1 π-bonded chain, which is characteristic of the cleavage face, merely by exposing the surface to a short pulse of low energy electrons (2-10 eV) from the STM tip. Figure 2 shows a before and after set of tunneling images of this process. In Figure 2a are three double-layer steps running approximately along $\langle\bar{1}10\rangle$ with some residual debris (from the load locking procedure) visible. A small set of row-like features is visible on the extreme left; these are 2x1 chains from an exposure performed previously. In Figure 2b, subsequent to a short e-beam exposure at 6 eV, a new 2x1 domain at the center of the image is clearly seen along with the domain present in the previous image. This new domain is approximately 60 x 80 Å in extent and has the electronic characteristic of the Si(111)-2x1 as demonstrated by the tunneling spectra shown in Figure 3. In this figure, the current-voltage characteristic of the tunnel junction over selected surface features is plotted as the normalized conductivity, $(dI/dV)/(I/V)$. This quantity is roughly proportional to the local density of states. The upper spectrum is typical of the H-terminated surface, displaying an energy gap of $\sim$1.2 eV, with broad features above and below this, characteristic of the indirect bulk bands of silicon. In sharp contrast is the data in the lower spectrum. Here, a number of sharp features are seen which extend into the energy gap of the H-terminated surface. These features are due to the surface states arising from the π-bonding inherent in the 2x1 surface structure [9, 10, 13]. Surprisingly, not only has the hydrogen been removed from the surface, but the underlying substrate has promptly reordered into a lower energy configuration.

A clue to the reaction mechanism may be obtained from the data in Figure 4 which shows the normalized 1x1 $\Rightarrow$ 2x1 conversion area as a function of incident electron kinetic energy [3]. This particular data is taken with STM feedback electronics in operation with only the endpoint bias varied. Since the tip retracts from the surface with increasing bias voltage in the Fowler-Nordheim regime in order to maintain constant electric field at the cathode surface, the geometrical area

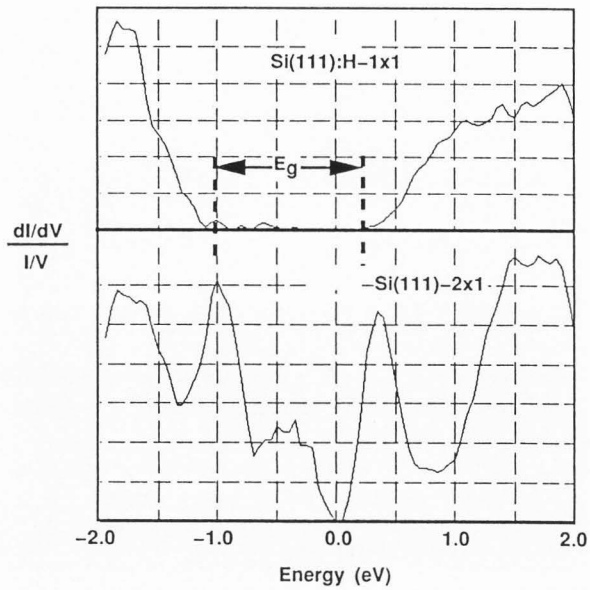

Figure 3. Tunnel junction spectrum of both the Si(111):H-1x1 and Si(111)-2x1 surfaces produced by electron stimulated desorption. This data is plotted as the normalized conductivity, with the vertical scale arbitrary. The energy scale designates position with respect to the sample Fermi level. The surface energy gap is denoted for the hydrogen terminated surface. These spectra are acquired at 100 pA demanded tunneling current using the interrupted feedback loop method.

---

illuminated by the field emitted electrons increases with the square of the tip-sample separation. This quantity is measured during the acquisition of this data and subsequently used to normalize the 1x1 ⇒ 2x1 conversion area. A peak is visible at ~6 eV, with an upturn in efficiency as the kinetic energy is increased beyond 10 eV. The peak is resonant with the indirect gap between Si-H bonding and antibonding bands, indicating the reaction path is one of promoting an electron from the bonding to the antibonding band. The cross-section for this is quite low; approximately 10^8 electrons are required for each surface site converted. Theoretical calculations on the Si(111):H surface suggest the Si-H σ and σ^* bands are separated by approximately 6 eV [12]; however, no strong bands are present at the Γ point. For these reasons, any resonant condition is expected to be broad and weak, as suggested by the data in Figure 4. As the electronic kinetic energy is increased significantly beyond 10 eV, secondary electrons may be created translating the interaction to the low side of the curve. Indeed, as the kinetic energy is raised beyond 20 eV, the 2x1 conversion region rapidly extends beyond that illuminated by simple geometric considerations, indicating that other mechanisms come into play. Nevertheless,

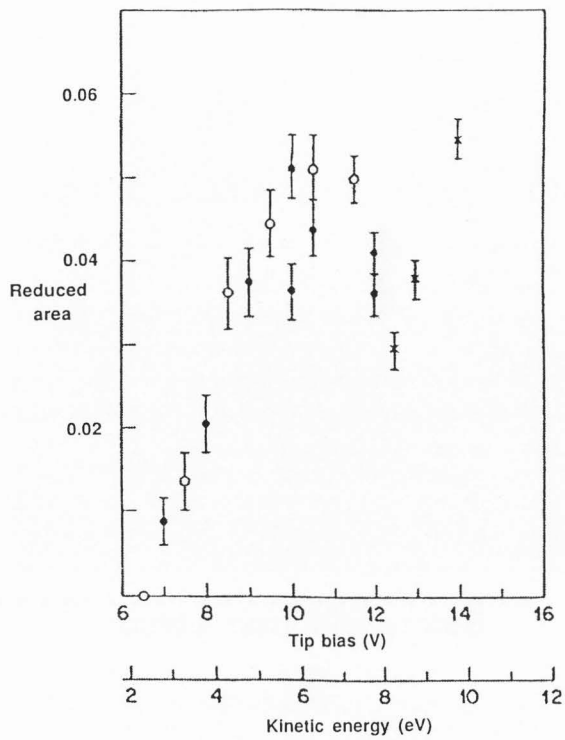

Figure 4. Reduced conversion area plotted against endpoint bias for the electron stimulated desorption of atomic hydrogen from Si(111). The various symbols designate different data runs, while the error bars are derived from the total converted areas.

---

the presence of the peak in conversion efficiency at ~6 eV argues against simple heating of the substrate by the field-emitted electrons, for, in this case, a monotonically increasing conversion area is expected.

This set of measurements demonstrated the power of the vacuum STM to induce simple chemical reactions at isolated regions on a sample surface at the atomic level. While it is clear that the H-termination is removed by the electron bombardment, it is unclear whether all of the hydrogen must be eliminated or only a smaller, critical number density which results in a local configuration with a greater unsatisfied dangling bond density than may be tolerated. Under these conditions, the substrate reconfigures to the 2x1, desorbing the remaining hydrogen in the process since the presence of Si-H bonds are inconsistent with the π-bonding of the 2x1. It may be further instructive to ask what other changes occur to the substrate during the electron stimulated desorption of the terminating hydrogen.

Figure 5 shows the final 2x1 surface after H-desorption for both flat (a) and stepped (b) substrates. In both cases, we see that the surface is divided into domains corresponding to the three twinned orientations allowed

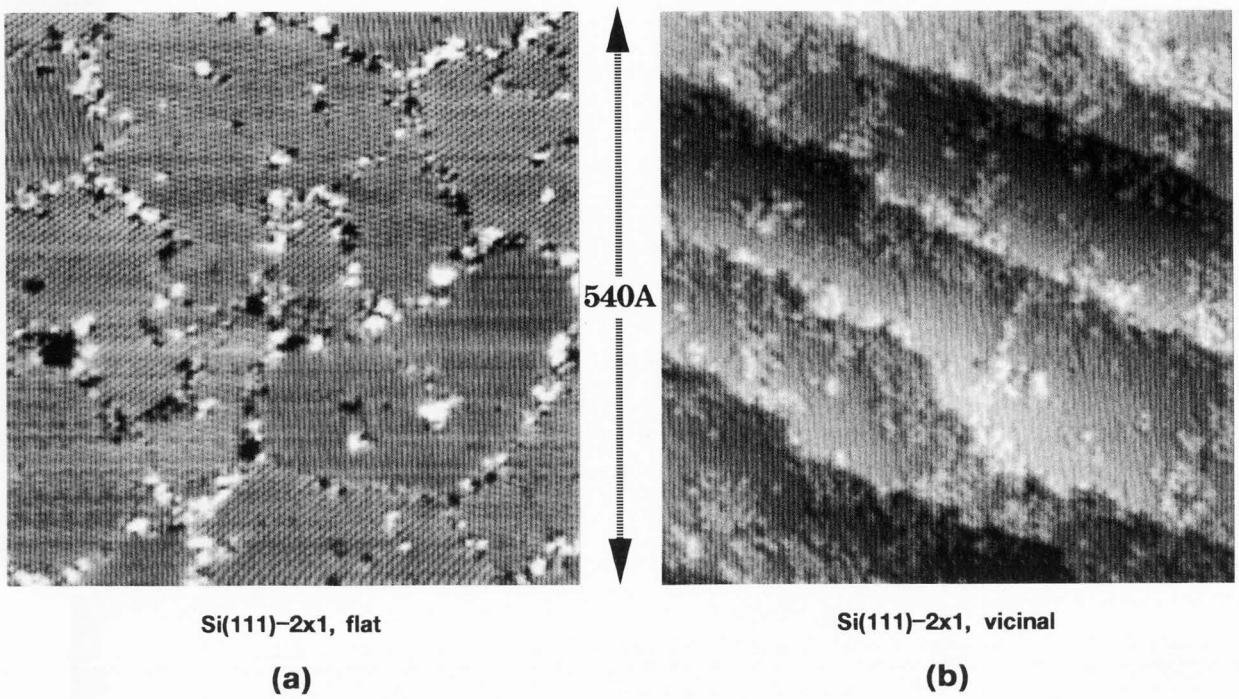

Figure 5. (**a**) Flat and (**b**) stepped Si(111) surfaces after electron stimulated desorption from the STM tip. Note the greater amount of surface adatoms for the stepped sample which was miscut at 1.25° toward $\langle\overline{1}12\rangle$. Both images were acquired tunneling into unoccupied sample states at +2.0 V bias.

---

on a (111) surface. Unlike the 2x1 surface created by cleavage, where typically only one domain orientation is present, the 2x1 surfaces left after hydrogen desorption are broken up into a number of individual domains with a typical size of 200 Å, with observed upper limit of ~400 Å. Figure 5a is typical of the domain distribution for "flat" (vicinality < 0.2°) Si(111) surfaces, with sizes ranging from ~100 Å up to 300 Å. As expected, the domains are distributed equally between the three possible orientations. For the vicinal surfaces, typified by the image shown in Figure 5b, the domain size is restricted by the mean distance between step risers imposed by the misorientation. For the image in Figure 5b, the miscut angle of 1.25° toward $\langle\overline{1}12\rangle$ forces double-layer steps an average of 145 Å; fluctuations and polishing roughness generate situations where the step-step spacing is both as close as 100 Å and as dispersed as 250 Å. From these considerations, this vicinality is just large enough for the presence of the step array to influence the 2x1 domain distribution. Figure 6 shows a set of tunneling images covering a lateral extent of ~1000 Å where the 2x1 structure has been created on another substrate misoriented 1.25° toward $\langle\overline{1}12\rangle$. Analysis of this image, and others like it, show that the presence of the step array has altered the distribution of 2x1 domains; the domain comprised of π-chains parallel to the step risers, $D_{\equiv}$, is suppressed to the point that only 10 per cent of the step risers consist of this orientation, while the two domains whose chains intersect the step riser at 60°, $D_{\perp}$, are enhanced, both comprising 45 per cent of the step riser. This result is a bit surprising in view of the fact that step terminations where the π-chains are parallel to the step riser are both simple in atomic configuration and expected to be locally favorable [4]. If the vicinality is increased to 2.5°, the $D_{\equiv}$ domains are virtually eliminated.

Close inspection of the tunneling image in Figure 6 shows that in many cases the $D_{\equiv}$ domains are larger in extent near the upper step riser and attenuated as they near the lower step riser. One such region may be seen in the lower left of Figure 6. Examination of many such images show this as generally true; as the proximity of the lower step riser decreases, the $D\perp$ domains on either side swallow the $D_{\equiv}$ domain. What is most likely occurring is an interaction between the anisotropic strain fields introduced by the presence of the 2x1 reconstruction and the step array which breaks the degeneracy of the three domain orientations. Calculations by Vanderbilt [18] show that the 2x1 π-chain surface is in tension both along and across the chains, but greater

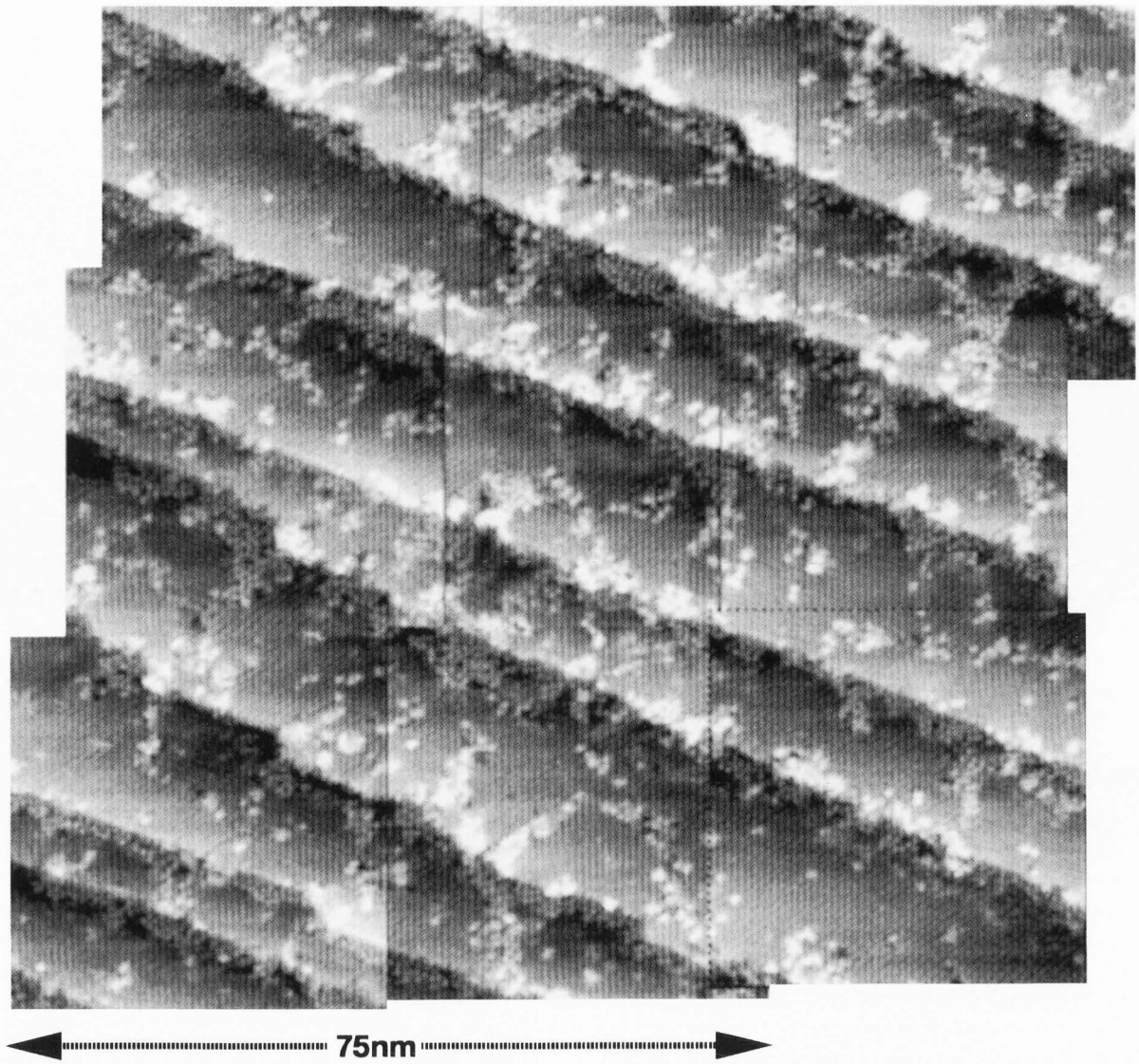

Figure 6. Large scale image of hydrogen desorbed Si(111) surface showing the relationship among step risers, adatoms, and the various 2x1 domains. These images were acquired at +2.0 V bias, tunneling into unoccupied sample states.

tension exists along the chains rather than across. Since the step risers represent a place on the surface where the atomic configuration may be relaxed by a small amount, it is more favorable to orient the chains in a manner whereby the greatest strain may be satisfied. For the flat substrates, the step risers are separated by more than the 2x1 domain size causing an equal distribution among the three domains since this represents, on average, isotropic stress.

Finally, one may legitimately ask if the silicon itself undergoes any reaction during the desorption of the hydrogen. Inspection of the data in Figure 5 shows that there are more isolated surface atoms (adatoms) on the stepped 2x1 surface than the flat surface, as is also true in Figure 6. Figure 7 shows a comparison of Si(111):H stepped surface, and a similar Si(111)-2x1 stepped surface after H-desorption. There are a large number of additional adatoms, and the step risers are themselves ragged and uneven. Examination of a number of images like those shown in Figure 5-7 indicated that approximately half of the step edge atoms are desorbed from the step risers and diffuse out over the lower terrace, many concentrated in the region immediately adjacent to the upper terrace step riser as shown in Figure 8. Further examination of the tunneling image in Figure 8 reveals that the silicon adatoms are not randomly arrayed but

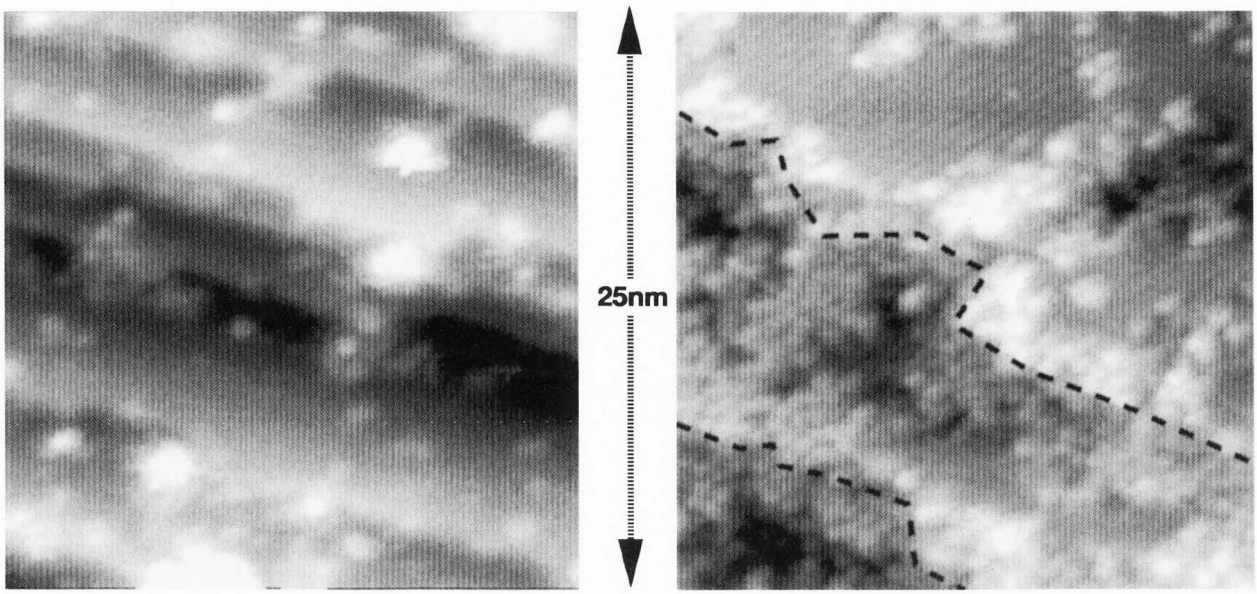

Figure 7. Tunneling images of stepped Si(111):H (**a**) and the equivalent stepped hydrogen desorbed surface (**b**). The dashed lines in (**b**) denote the location of the step riser. Both images were taken tunneling into unoccupied sample states at +2.0 V bias. The miscut is along $\langle\overline{1}12\rangle$ with an angle of 2.5° in (**a**) and 1.25° in (**b**).

Figure 8. Stepped hydrogen desorbed Si(111) surface showing the deconstruction of the 2x1 regions into 2x2, c4x2 adatom structures as denoted by the arrows. This image was taken tunneling into unoccupied sample states at +2.0 V bias.

are organized in 2x2 and c4x2 configurations similar to those found on the Ge(111) surface. Bias-dependent tunneling images taken on both sides of the surface energy gap, such as those shown in Figure 9, demonstrate that the substrate in these adatom decorated areas no longer consist of the 2x1 π-chains but have been transformed to a 1x1 arrangement with adatom decoration in a 2x2 geometry. These areas are denoted by the adatoms (white balls) designated with x's. Upon deconstruction of the substrate, a charge transfer is set up between the dangling bonds residing on the adatoms and those residing on substrate restatoms, resulting in a mismatch in registration between the image sets [2]. Adatoms which are either not in sufficient local density to cause substrate deconstruction or are in local $\sqrt{3} \times \sqrt{3}$ geometries (such as the triangle near the center) show no such mismatch. While no data exists as yet bearing on the sequence of the reaction, the following scenario seems likely: (**1**) hydrogen desorbs from the terraces and step risers under electron bombardment; (**2**) step edge silicon atoms become mobile during this phase and diffuse out over the lower terrace; (**3**) the remaining hydrogen desorbs during the phase transition to the 2x1; (**4**) the silicon adatoms diffuse to the domain boundaries (or cause them); and (**5**) at a critical adatom concentration

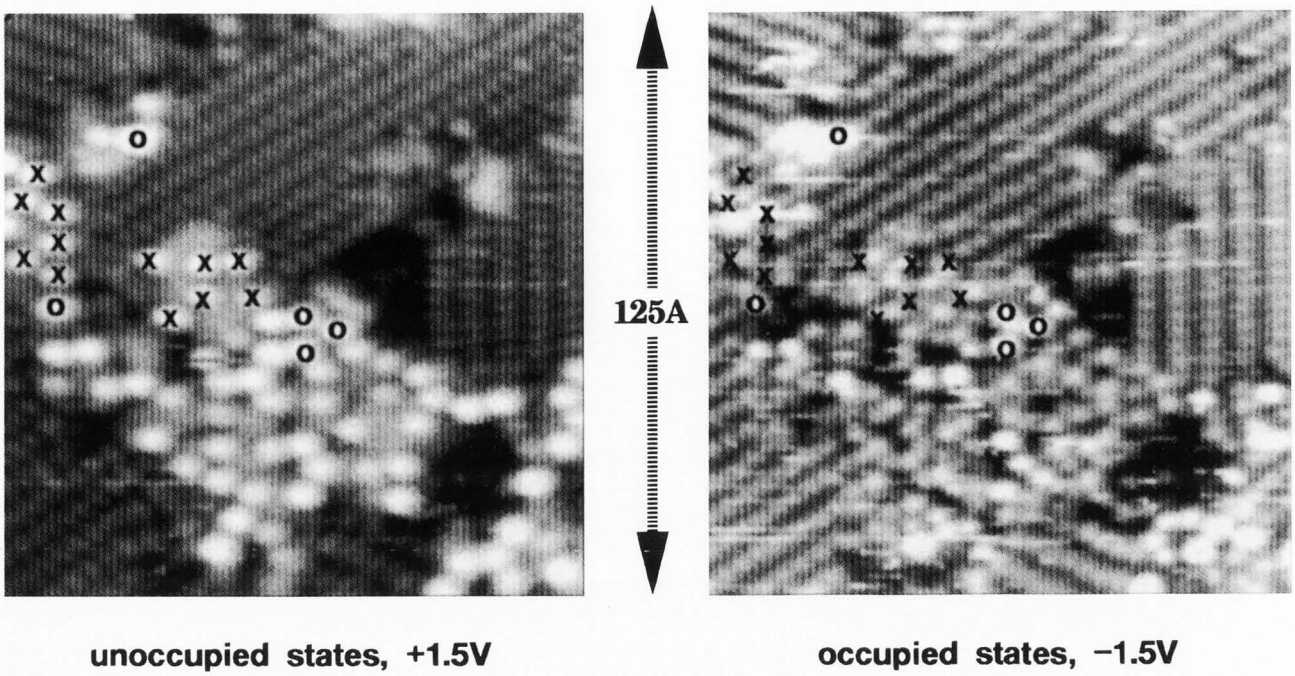

Figure 9. Dual polarity tunneling images of the hydrogen desorbed Si(111) surface with the bias conditions as shown. The x's denote adatoms which have reconstructed the underlying 2x1 π-chains into 2x2 adatom structures, while the o's denote similar adatoms which are either insufficient in a real density to cause the restructuring of the substrate or locally in $\sqrt{3}$ configuration resulting in registration between the two images.

(~0.25 monolayer), the 2x1 is itself transformed to a 2x2 adatom phase. We can see from this that even simple atomic desorption may generate a complex sequence of events on the substrate material. Further, these observations conclusively demonstrate that the Si(111)-2x1 structure is energetically unfavorable to small areas of the 2x2 adatom phase in the presence of a source of adatoms.

Conclusion

In summary, the STM is a powerful tool for the study of simple chemical reactions on an atomic level. It may be used not only to observe the results of reactions such as gas adsorption and other material deposition but also to stimulate species on suitable surfaces to undergo reactions of which the results may then be observed. Observation of the electronic and geometric configuration of the substrate before and after the desorption suggest that a complex series of events takes place for even the simplest processes.

References

[1] Becker RS, Golovchenko JA, McRae EG, Swartzentruber BS (1985) Tunneling images of atomic steps on the Si(111)7x7 surface. Phys. Rev. Lett. **55**, 2028-2031.

[2] Becker RS, Swartzentruber BS, Vickers JS, Klitsner T (1989) Dimer-adatom-stacking. Phys. Rev. B **39**, 1633-1647.

[3] Becker RS, Chabal YJ, Higashi GS, Becker AJ (1990) Atomic scale conversion of clean Si(111):H-(1x1) to Si(111)-(2x1) by electron-stimulated desorption. Phys. Rev. Lett. **65**, 1917-1920.

[4] Feenstra RM, Stroscio JA (1987) Reconstruction of steps on the Si(111)-2x1 surface. Phys. Rev. Lett. **59**, 2173-2176.

[5] Higashi GS, Chabal YJ, Trucks GW, Raghavachari K (1990) Ideal hydrogen termination of the Si(111) surface. Appl. Phys. Lett. **56**, 656-658.

[6] Klitsner T, Becker RS, Vickers JS (1991) Initial stages of oxidation of Ge(111)-c(2x8) studies by scanning tunneling microscopy. Phys. Rev. B **44**, 1817-1824.

[7] Leibsle FM, Samsavar A, Chiang T (1988) Oxidation of Si(111)7x7 as studies by scanning tunneling microscopy. Phys. Rev. B **38**, 5780-5783.

[8] Ol'shanetskii BZ, Makrushin NI, Volokitin AI (1973) Low-energy electron diffraction from a (111)

germanium suface during the early stages of oxygen adsorption. Sov. Phys. Sol. St. **14**, 2713-2716.

[9] Pandey KC (1981) New Pi-bonded chain model for Si(111)-(2x1) surface. Phys. Rev. Lett. **47**, 1913-1916.

[10] Pandey KC (1982) Reconstruction of semiconductor surfaces: Buckling ionicity, and the Pi-bonded chain. Phys. Rev. Lett. **49**, 223-226.

[11] Peltz JP, Koch RH (1991) Successive oxidation stages and annealing behavior of the Si(111)7x7 surface observed with scanning tunneling microscopy and scanning tunneling spectroscopy. J. Vac. Sci. Tech. **B9**, 775-778.

[12] Schluter M, Cohen ML (1978) Nature of conduction-band surface resonances for Si(111) surfaces with and without chemisorbed overlayers. Phys. Rev. B **17**, 716-725.

[13] Stroscio JA, Feenstra RM, Fein AP (1986) Electronic structure of the Si(111)2x1 surface by scanning-tunneling microscopy. Phys. Rev. Lett. **57**, 2579-2582.

[14] Stroscio JA, Feenstra RM, Fein AP (1987) Local state density and long-range screening of adsorbed oxygen atoms on the GaAs(110) surface. Phys. Rev. Lett. **58**, 1668-1671.

[15] Takayanagi, Tanishiro Y, Takahashi M, Takahashi S (1985) Structural analysis of Si(111)-7x7 by UHV-transmission electron diffraction and microscopy. J. Vac. Sci. Tech. **A3**, 1502-1506.

[16] Tersoff J, Hamann DR (1983) Theory and application for the scanning tunneling microscope. Phys. Rev. Lett. **50**, 1998-2001.

[17] Tokumoto H, Miki K, Murakami H, Bando H, Ono M, Kajimura K (1990) Real time obsercation of oxygen and hydrogen adsorption on silicon surfaces by scanning tunneling microscopy. J. Vac. Sci. Tech. **A8** K, 255-258.

[18] Vanderbilt D (1987) Absence of large compressive stress on Si(111). Phys. Rev. Lett. **59**, 1456-1459

[19] Wolkow RA, Avouris Ph (1988) Atom-resolved surface chemistry using scanning tunneling microscopy. Phys. Rev. Lett. **60**, 1049-1052.

Discussion with Reviewers

Reviewer III: It is confusing to compare the energetics of equilibrium reconstructions on different surfaces. Are the authors referring to the inferior long-range coherence of the Ge(111)-c2x8 compared with the Si(111)-7x7?

Authors: We are referring to the fact that the c2x8 on Ge(111) is a simple adatom phase composed of two distinct subunits with c4x2 and 2x2 symmetry arranged coherently to form the c2x8. Together, these simpler structures may be considered a 2x2 adatom phase with little rearrangement of atoms in the layer immediately below the adatom layer. This is in distinction to the 7x7 dimer-adatom-stacking fault (DAS) structure found on Si(111) which may only be simple decomposed into the faulted and unfaulted mesh halves and, by virtue of its partial stacking fault, involves considerable rearrangement of subsurface atoms. Since comparatively little free energy difference exists between the various Ge(111) adatom structures, the Ge(111) surface employs at least three surface phases, the c2x8, c4x2, and 2x2, to accommodate defects and steps. In contrast, the 7x7 found the Si(111) surface has a considerably lower free energy than related phases such as a simple 2x2 adatom phase to the point that even atomic steps are rearranged to accommodate the 7x7, and thus there is a smaller diversity of reaction sites. We have always found it useful to compare reactions on germanium and silicon surfaces since both materials are elemental semiconductors with very similar band structure.

Reviewer III: The emphasis in the section on the authors' original work is on the description of the new phenomenon of deconstruction accompanying desorption. It would be useful to make the experimental procedure more explicit. How long are the short voltage pulses? Does the converted area depend on the rise time or the duration of the pulse? Are these controlled parameters?

Authors: The short pulses are ~ 1 sec in duration (given the cross-section for desorption, short is only a relative term). The rise time is not meaningful in this experiment, since the voltage is ramped up from the tunneling bias (~ 2 V) up to the demanded endpoint bias (5-10 V) with the STM feedback loop engaged. For these reasons, the slew rate must be less than the STM bandwidth. For our STM, this results in a slew rate of 3-5 V/sec, in order to maintain constant current, which is important when later normalizing the conversion areas. All of the parameters are of necessity controlled, with tunneling/field emission current held at 1 nA.

Reviewer III: In a similar spirit, why is the energy scale in the I-V spectra (Figure 3) arbitrary? Is the offset also arbitrary?

Authors: The energy scale is clearly marked along the bottom of the lower plot (serving for both) and ranges from -2.0 eV (2 eV below the sample E_F) and +2.0 eV. The scale for the signal, $(dI/dV)/(I/V)$, is not marked (and thus arbitrary). This is because the absolute value of this derived quantity depends on the curvature of the STM tip, with different tips giving different absolute numbers at the bias endpoints (generally ranging between 3 and 7). The value at the origin, 0.0, is zero

due to a small offset added to I/V in order to avoid divergence arising from limits on signal-to-noise in the neighborhood of the origin. This arises from the fact that at 0 V bias, no current flows and the signal-to-noise diverges.

T. Klitsner: How confident are the authors of the peak in the desorption area versus tip bias data in Figure 4? Does the fact that the tip changes its height above the surface as a function of bias greatly complicate this analysis? How is the tip height measured, and how accurate is this determination?

Authors: The peak in the reduced area is derived from three overlapping data sets on two samples and is obvious even before the normalizing of the areas. The changing tip height is a minor complication because it is routinely measured in the course of all spectroscopic measurements made in our lab. The relative tip heights are determined simply by recording the feedback error signal while ramping the tip bias. The initial tip height, z_0, is determined by fitting the electron standing wave/barrier resonance spectrum to a theoretical one-dimensional tunneling model. The frequency of the resonances above the vacuum level is a sensitive function of the initial tip-sample separation since these surfaces form a Fabry-Perot for the field-emitted electrons. For these reasons initial tip height error is always less than 1 Å, and generally less than 0.5 Å. The total excursion of the tip is $\sim$25 Å during a single measurement.

T. Klitsner: Could there still be hydrogen on the post-desorption 2x1 regions, which would create a non-π-bonded, H-terminated 2x1 structure on Si(111)?

Authors: This scenario is unlikely. First, the I-V spectrum we record on the 2x1 regions is nearly identical to that reported by Feenstra and Stroscio [4] in their extensive study of the π-bonded chain Si(111)-2x1 surface. Further, dual polarity STM images, similar to those shown in Figure 9, show the same phase shifts between images taken above and below the surface energy gap in both the $\langle 1\bar{1}0 \rangle$ and $\langle 2\bar{1}\bar{1} \rangle$ directions as those published by Feenstra and Stroscio [4]. Finally, the presence of hydrogen saturating the dangling bonds on the Si(111) surface would remove the driving force, i.e., the π-bonding, responsible for the formation of the chain.

T. Klitsner: The authors state that their observations demonstrate the Si(111)-2x1 structure is unstable with respect to a source of adatoms. Does this mean that deposition of silicon onto this surface would convert this surface into an adatom phase?

Authors: Not at room temperature. The presence of the extra Si atoms at the lower edge of the atomic steps shows that the Si edge atoms are desorbed at, or close to, the same time as the desorption of hydrogen from the terraces. Regions where the (111) double-layer has a sufficient quantity of adatoms (from the nearby step riser) will reconstruct as an adatom phase, while those regions further from the step risers, by inspection 15-20 Å, will reconstruct as 2x1 π-chains.